Available online at www.sciencedirect.com
ScienceDirect
Journal of the European Ceramic Society 26 (2006) 3631–3638
www.elsevier.com/locate/jeurceramsoc

Room temperature synthesis of chitosan/apatite powders and coatings

J. Peña [a], I. Izquierdo-Barba [a], M.A. García [b], M. Vallet-Regí [a,b,*]

[a] *Departamento Química Inorgánica y Bioinorgánica, Facultad de Farmacia, UCM, 28040-Madrid, Spain*
[b] *Instituto de Magnetismo Aplicado, UCM-CSIC-RENFE, Las Rozas, P.O. Box 155, 28230-Madrid, Spain*

Received 28 September 2005; accepted 9 December 2005
Available online 20 March 2006

Abstract

Bioactive chitosan/apatite powders and adherent coatings have been synthesized by a co-precipitation method and an alkaline transformation at room temperature. Powders with organic/inorganic ratios ranging from 42 to almost 90% can be prepared in substantial amounts. This method allows to coat Ti6Al4V substrates yielding films with thicknesses of approximately 1 μm that show an adhesion strength superior to 15 MPa. The coating procedure can be repeated to increase the thickness of the layer. The formation of apatite onto these materials after immersion in a simulated body fluid (SBF) indicates a potential bioactivity in vivo. The materials have been characterized by viscosimetry, XRD, FTIR, SEM, EDS and TG/ATD. The adhesion strength was determined by a pull-out test.

Keywords: Films; Sol–gel processes; Apatite; Biomedical applications

1. Introduction

The nature-inspired self-assembly techniques are based on the interaction between the organic template and the inorganic filler, affecting, for example, to the controlled nucleation and crystal growth of the inorganic part or to the orientation of the organic components to form a higher order hierarchical structure. In this sense, the combination of a calcium phosphate with a great number of different polymers constitutes a growing field of research for bone/cartilage substitution.

Chitosan–calcium phosphate composites may result of great interest in orthopedic/periodontal applications[1–3] due to the outstanding properties of chitosan.[4–7] Chitosan is a biodegradable mucopolysaccharide formed by the β(1,2) linkage of 2 acetamido-2-desoxy-β-D-glucopyranose and 2-amino-2-desoxy-β-D-glycopyranose, obtained by deacetylation of chitin, the second most abundant biopolymer on earth and found mainly in invertebrates, insects, marine diatoms, algae, fungi, and yeasts. Chitosan has a great number of uses in completely different disciplines such as cosmetics, photography, water engineering, textile industry, paper finishing, food and nutrition, solid-state batteries . . .. Focusing on the biomedical field, chitosan and its derivatives have a great number of applications ranging from wound dressings, contact lenses, sorbents and enzyme supports, drug delivery systems, tissue engineering . . .. In particular, chitosan uses in the pharmaceutical industry are growing continuously not only in aspects related with controlled release from different delivery systems: microparticules, liposomes, vesicles, gels, suspensions . . . through diverse routes: oral, nasal, parenteral, transdermal . . ., but also in others such as fat trapper, excipients . . ..[8–9]

This great number of applications can be explained by considering the outstanding properties of chitosan and its derivatives when interacting with the human body: bioactivity, antimicrobial activity, immunostimulation, chemotactic action, similitude with extracellular matrix components such as glycosaminoglycans, enzymatic biodegradability, mucoadhesion and epithelial permeability . . ., which supports the attachment and proliferation of different cell types.[10–12]

Many authors have worked in the preparation of mixtures of calcium phosphates and chitosan in the form of powder,[13] membranes,[14,15] pastes,[16] cements,[17,18] scaffolds[19–22] or microspheres.[23–25] However, fewer publications focus on the preparation of both components at the same time which a priori should ensure a more intimate contact between them.[26–30]

The aim of this work is to obtain chitosan/calcium phosphate materials in the form of powders or coatings at room temper-

* Corresponding author. Tel.: +34 91 394 18 61; fax: +34 91 394 17 86.
E-mail address: vallet@farm.ucm.es (M. Vallet-Regí).

0955-2219/$ – see front matter © 2006 Elsevier Ltd. All rights reserved.
doi:10.1016/j.jeurceramsoc.2005.12.028

ature. The key factor consisted on finding a precursor solution from which both forms could be obtained. In this sense, citric acid has a crucial role in the preparation of these materials: it allows to dissolve chitosan and, due to its chelating nature, to prepare concentrated solutions containing calcium and phosphate with enough stability as to prepare powders or coatings. In addition, citric acid along with chitosan facilitates the formation of layers due to its properties as film former, attributable to its ability to enhance gelation improving the wettability of a coating solution on a substrate. In fact, it has been employed as an additive in the preparation of apatite films or powders by sol–gel.[31]

Nowadays, the most frequently employed technique to prepare commercial covered implants is plasma spray.[32] However, it has some disadvantages that cannot be easily avoided: unable to coat implants with complex shapes, differences in the chemical composition, delamination …. Other line-of-sight deposition methods such as sputtering or laser ablation do not solve, for instance, the coating of porous substrates.[33,34] Alternatively, solution-based methods are an emerging option for the preparation of these coatings due to several features: better control of coating morphology, chemistry and structure, covering of intricate pieces, simple of technology . . . future directions[35,36] aim at coating methods that ensure osteoconductive properties and the ability to deliver therapeutic agents, growth factors, adhesion proteins, adhesion peptides … and, even, act as cell support for tissue engineering. Biomimetic-inspired methods[37–42] fulfill some of these requirements, although there are still some concerns that must be improved such as the adhesion of the coating or the deposition time. Electrodeposition/electrophoretic methods followed by an alkaline treatment of the so obtained brusite coatings instead of a thermal treatment aim also at this direction.[43–45]

The synthetic method employed in this work combines the sol–gel approach with the advantages of the scarce room temperature techniques such as mineralization or electrochemical deposition. However, the following differences must be outlined: the precursors employed are low cost and do not contain harmful or undesired residues that are usually eliminated by a subsequent thermal treatment; in fact, this annealing process is not compulsory and allows the presence of chitosan with the calcium phosphate and the introduction of substances with potential therapeutic effects during the coating process. The inclusion of this type of compounds in calcium phosphate layers is not an easy task and has been solved in a biomimetic-inspired second stage in which the already prepared films or the induced Ca/P deposition layers are immersed in a simulated body fluid (SBF) that contains the substance.[46–49] The option of introducing larger and well-known amounts in one coating step is a promising possibility.

2. Experimental section

The synthesis route utilized to prepare both types of materials is schematised in Fig. 1. Both processes have in common the precursor solution, which only differentiates in the superior amount of citric acid added to ensure the stability of the solution during the deposition procedure.

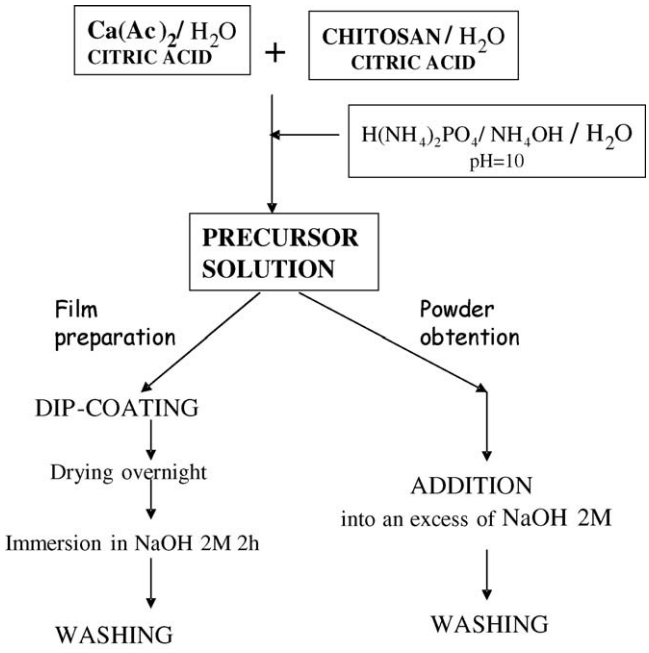

Fig. 1. Scheme of the synthetic route employed.

2.1. Precursor solution preparation

The solutions employed to prepare powder or films only differ in the amount of citric acid added, i.e. a higher carboxylic acid/calcium source ratio was employed to cover the substrates. A higher quantity of citric acid contributes to the stability of the solution (∼12 h) required to prepare the films. In the case of powder preparation this factor has no significance since the successive addition of the P source and NaOH produces the precipitation of the chitosan–apatite material.

2.2. Powder synthesis

Different compositions of powder were prepared by increasing the quantity of Ca and P sources and maintaining the chitosan content (Table 1). In all cases a Ca/P ratio of 1.667 is maintained. For example, in order to prepare sample D, 15.816 g of $Ca(Ac)_2$ is added into an aqueous solution of citric acid. Meanwhile 1 g of chitosan is added in water containing citric acid and left overnight to ensure its adequate solution. The total volume of water employed in both solutions adds up to 100 ml. Subsequently, the solution containing the calcium acetate is poured in the chitosan/citric acid solution and stirred for 1 h; followed by the addition of 100 ml containing 7.92 g of $H(NH_4)_2PO_4$ in water with a pH 10 (by NH_4OH addition). The precipitate formed while adding the P source redissolves immediately yielding a solution. This solution is stirred for another hour and slowly poured into a 2 M NaOH aqueous solution, the pH is maintained over 11 by addition of further NaOH 2 M solution. The so obtained precipitate is washed repeatedly until a neutral pH is detected.

Table 1
Nomenclature and composition of the precursor solutions

	Ca source solution			P source solution $[H(NH_4)_2PO_4]$ (M)
	$[Ca(Ac)_2]$ (M)	Citric acid:$[Ca^{2+}]$ ratio	Chitosan content (mg/ml)	
0	–	1:1	10	–
A	0.125	1:1	10	0.075
B	0.250	1:1	10	0.150
C	0.500	1:1	10	0.300
D	1.000	1:1	10	0.600
E	2.000	1:1	10	1.200
Coating preparation	1.000	4:1	10	0.600

2.3. Film deposition

Dipping was carried out by means of a device designed and implemented at the Condensed Matter Physics Department of Universidad de Cádiz. Ti6Al4V rods with dimensions 12 mm × 1 mm were abraded with a 320 silicon grit range carbide paper, polished with 9, 3 and 1 μm diamond paste and washed with distilled water, alcohol and acetone. The substrates were extracted at a rate of 1000 μm/s and dried in air overnight. The obtained coatings were immersed in NaOH 2 M for 2 h.

2.4. Characterization

Fourier transform infrared (FTIR) spectra were obtained in a Nicolet Nexus spectrometer equipped with a smart golden gate ATR accessory. The crystallinity of the materials was analyzed by X-ray diffraction (XRD) in a Philips X-Pert MPD diffractometer equipped with a thin film attachment. The fixed incidence angle was 1° for all samples. Surface morphology was analyzed by scanning in a JEOL 6400 electron microscopy (SEM). The thickness estimation was performed by cross-section examination of layers previously embedded in a EPOTHIN resin. The Ca and P content was determined by energy dispersive spectroscopy (EDS) using a LINK 10000 analyzer on samples covered with graphite. The topography of the samples was obtained by using an Autoprobe-CP SFM from Park Scientific Instr working in contact mode. Cantilevers with a 0.4 N/m force constant and conical tip were used. Viscosity measurements were carried out in a Haaker Reostress rs75 rheometer to characterize the precursor solutions. Thermogravimetry (TG) and differential thermal analysis (DTA) were performed in a Perkin Elmer Pyris Diamond TG/DTA analyser, with 10 °C/min heating ramps.

In vitro tests were carried out by soaking the covered substrates, vertically mounted in a platinum scaffold, in 10 ml of SBF,[50] at 37 °C, in sterile polyethylene containers in sterile conditions. Soaking periods were 3, 7, 15 and 30 days.

The adhesive strength was measured by the pull-out test, in accordance with American Society for Testing Materials (ASTM) specifications:[51] a pair of metallic jigs were bonded to the coated and the uncoated titanium substrates, these ensembles were joined by means of the loctite 480 adhesive. After leaving the set for 1 day, for complete curing of the adhesive, the adhesive strength of the film was measured by applying a tensile stress using a universal mechanical tester Microtest SCM 3000 at a crosshead speed of 0.5 mm/s until fracture occurred. Five measurements were done for each data point.

3. Results and discussion

3.1. Chitosan/apatite powders

The obtained powders are white colored and show an increasing sheet-like macroscopic morphology with the chitosan/ceramic ratio. The XRD characterization shows that all the samples prepared can be identified as a low crystalline apatite (powder diffraction file 9-432 JCPDS 2000) which, studied by SEM, reveals to be formed by aggregates of small crystallites of several nanometers in size (Fig. 2). In addition, FTIR (Fig. 3) allows to appreciate the bands attributable to chitosan[52] and to hydroxyapatite;[53] the spectra of hydroxyapatite obtained under the same conditions without chitosan and that of chitosan without a ceramic content have been included in order to facilitate the assignation and interpretation of the infrared bands in the chitosan/apatite materials. The presence of chitosan complicates the characterization of the apatite obtained, as its bands overlap those that can be attributed to the presence of carbonate in the apatite structure. However, the study of the sample obtained without of chitosan shows bands attributable to the CO_3^{2-} ν_3 mode (1640, 1490, 1420–1415 cm^{-1}).[54] In addition, the appearance of a band at 875 cm^{-1} (CO_3^{2-} ν_2 mode), also noticeable in chitosan containing samples, confirms the presence of carbonate groups. Moreover, this band can also be attributed to the presence of HPO_4^{3-}, though no additional bands attributable to this anion (1210, 1130, 1099 cm^{-1}) can be detected. Due to the very low crystallinity of the samples prepared, the hydroxyl bands (3570 and 630 cm^{-1}) can be hardly appreciated, specially the last one.

The termogravimetric analysis allows to determine the amount of ceramic content within these materials; Fig. 4a shows the weight loss versus temperature indicating the residue percentage attributable to the ceramic content. In addition, the differential thermogravimetric analysis adds information about the way the organic part is eliminated, which depends on the degree of interaction between the ceramic and chitosan (Fig. 4b). A different decomposition process of the organic part can be

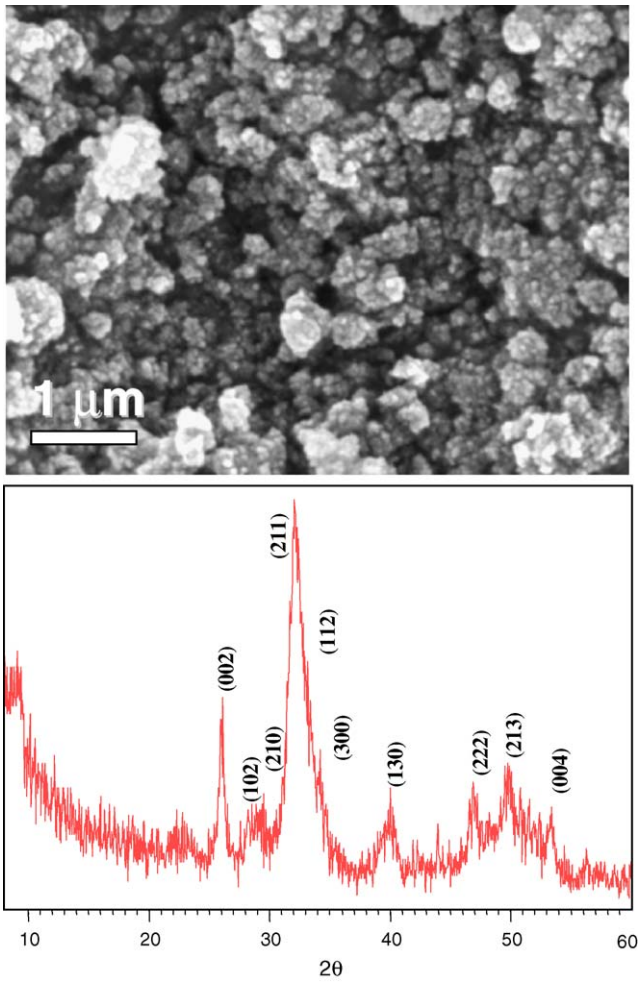

Fig. 2. SEM and XRD of sample D. Miller indexes correspond to hydroxyapatite.

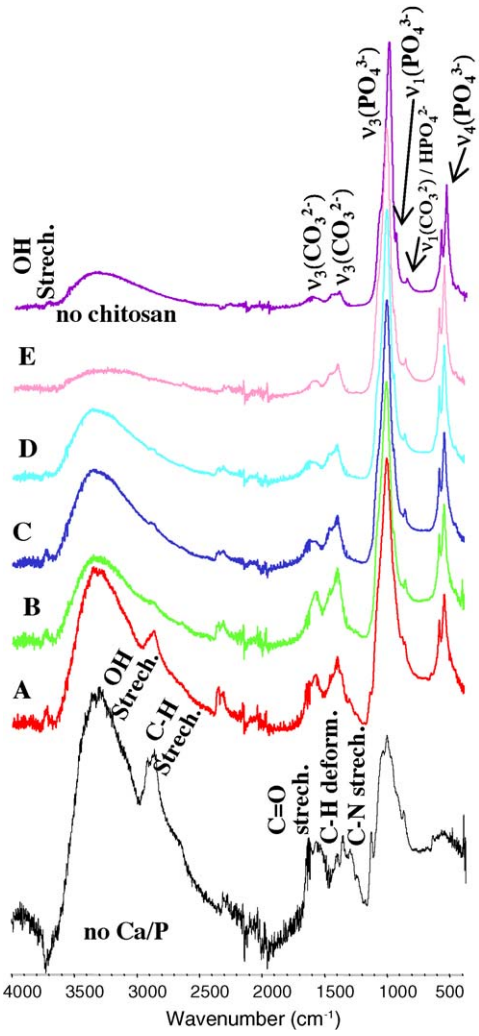

Fig. 3. FTIR spectra of the as-obtained powders.

distinguished between Ca/P containing and non-containing samples, i.e. the two exothermic peaks situated at 310 and 575 °C are shifted towards lower temperatures: 280 and 440 °C and a different decomposition pattern can be observed at these last temperatures without a clear single maximum, showing a continuous exothermic exchange instead. Among Ca/P containing samples, a progressive increase in the height of the 280 °C exothermic peak with the chitosan content can be detected as depicted in Fig. 4b inset. Fig. 4a also includes the XRD of a residue whose analysis may contribute to discern the nature of the low crystallinity crystals originally obtained. For example, the evidence of extra phases such as calcium oxide (powder diffraction file 37-1497 JCPDS 2000) or β-tricalcium phosphate (powder diffraction file 9-169 JCPDS 2000) indicates a Ca/P ratio higher or lower that 1.6667. In our case no extra phases can be detected, in fact, further thermal treatments show that the hydroxyapatite structure remains stable up to 1450 °C for sample D, without the presence of additional phases (data not shown).

Finally, it must be mentioned that the immersion in NaOH not only leads to the transformation into a poorly crystallized apatite but also to the elimination of considerable amounts of citric acid employed in this synthetic route and to the transformation of the chitosan $–NH_3^+$ into $–NH_2$, that, in turns, contributes to its stability.

In any case, the presence of citric acid has no negative effects at all, since it is a minor component of the bone, playing an important role in crystal growth/modification, and is present in many biochemical routes.[55] On the other hand, the influence of citric acid on the hydroxyapatite formation is still under discussion. Some authors claim that citrate favors the calcium phosphate phases nucleation but inhibits its growth, while others report an inhibition on the transformation of amorphous calcium phosphate to hydroxyapatite. Finally, other authors[56] have found that hydroxyapatite formation is not totally inhibited by citrate and that this ligand affects both the crystal size and the degree of perfection of the lattice cell, due to the inclusion of carboxyl groups.

In our case, citric acid allows, first, to dissolve chitosan and, also, ensures the stability of the precursor solutions at high concentrations even after phosphate source addition. Materials obtained from true solutions should yield a priori higher homogeneity when compared to those prepared from suspensions and much more so with respect to blends of ceramic and

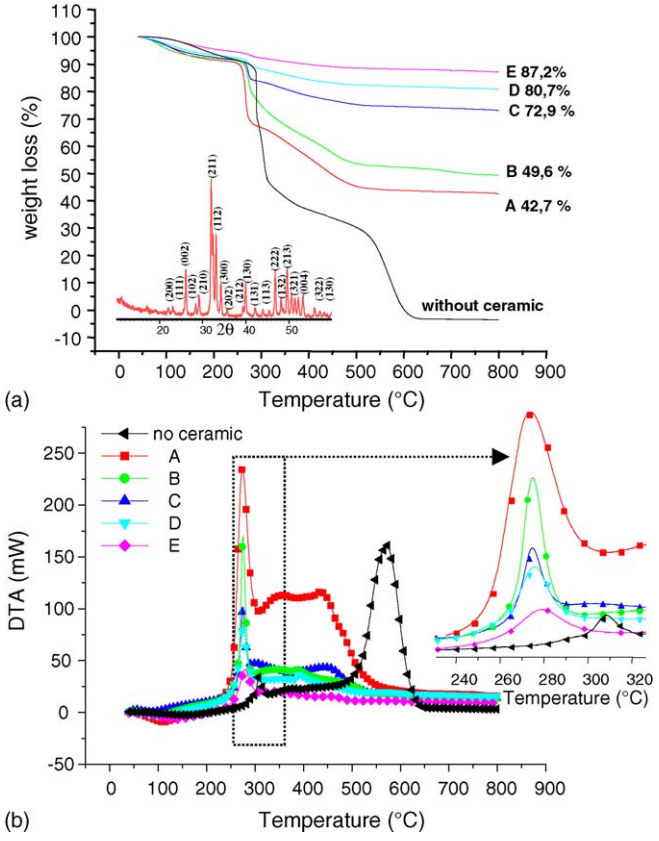

Fig. 4. Characterization of the obtained samples by (a) thermogravimetry, inset: XRD of sample D residue and (b) differential thermogravimetric analysis.

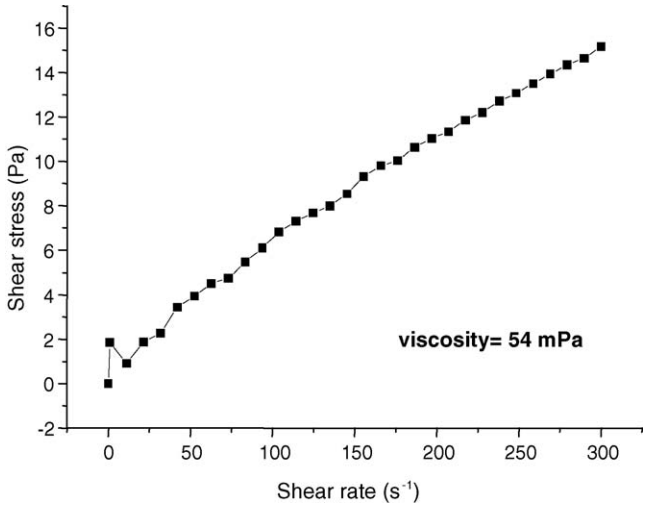

Fig. 5. Viscosimetry measurement of the precursor solution.

chitosan. In fact, as demonstrated by DTA, there is a strong interaction between the inorganic phase and the chitosan component. Besides, the chitosan content seems to contribute to the stability of the hydroxyapatite at high temperatures, i.e. in absence of chitosan, calcium oxide appears after annealing at 1000 °C, while it is necessary to reach 1450 °C to see the first evidences in sample D. This synthetic route allows to prepare highly concentrated precursor solutions when compared with similar methods such as those based on suspensions of $Ca(OH)_2$[26] and seems to be a simpler technique, with a different route and final goals, when compared with mineralization techniques of chitosan by successive immersing cycles in Ca and P source solutions.[27]

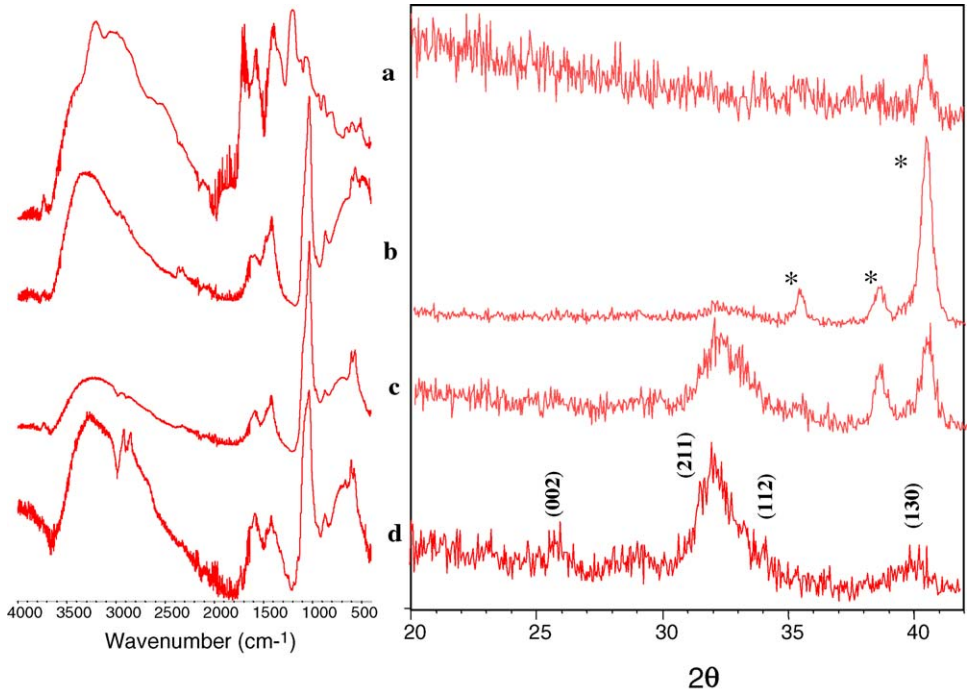

Fig. 6. FTIR and XRD of (a) non-NaOH treated; (b) one layer; (c) two layer; and (d) four layer coatings. Substrate maxima are marked as * and hydroxyapatite Miller indexes are displayed.

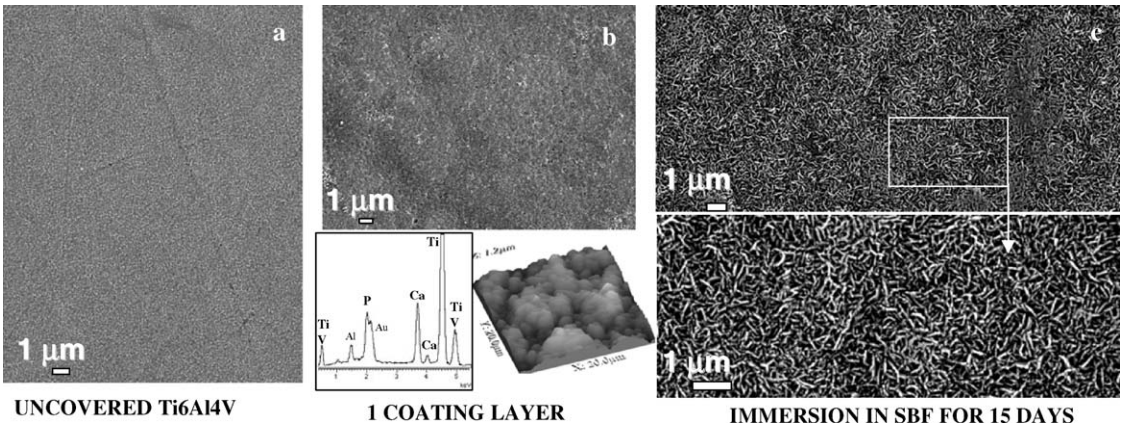

Fig. 7. SEM micrographs of (a) the Ti6Al4V substrate; (b) one coating layer, insets: EDS analysis, SFM micrograph; and (c) two different magnifications after 15 days immersed in SBF.

3.2. Chitosan/apatite coatings onto Ti6Al4V

In this work true solutions and not mere suspensions of powder in a solvent are employed to cover the substrates. However, in order to prevent a premature precipitation during the coating process, the precursor solution contains an extra quantity of citric acid (citric acid:Ca source 4:1) that helps to maintain the stability of the solution due to its chelation ability. In addition, citric acid shows a film-forming capacity that adds to that displayed by chitosan, due to its gelation-inducing porperties and, consequently, to improve the wettability of the coating solution on the substrate.

In this work, only solution D has been employed to prepare the coatings; however, the rest of the compositions detailed in Table 1 for powder preparation could, as well, be employed to coat substrates. The rheological characterization of this precursor solution shows a Newtonian-like behavior, with a viscosity value of 54 mPa (Fig. 5).

One of the advantages of this method is that a single coating can be performed within a short period of time. Consequently, thicker coatings can be prepared in almost no time by repeating the coating process (Fig. 1). Fig. 6 shows the XRD and FTIR spectra of Ti6Al4V substrates coated one, two or four times, as well as a monolayer coating non-NaOH treated. The FTIR spectra of the non-NaOH treated coating can be attributed to a mixture of citric acid, chitosan and calcium citrate, while the XRD diffraction hardly shows the maxima corresponding to the substrate. The treated layers show, when characterized by FTIR, besides the characteristic bands of chitosan, the more significant ones of phosphate (1040, 600 and 570 cm^{-1}) as well as that attributable to CO_3^{2-}/HPO_4^{2-} at 870 cm^{-1}. XRD shows the progressive disappearance of the substrate peaks and the presence of only the more intense maxima assignable to apatite: (0 0 2) and a broad peak that includes (2 1 1), (1 1 2), (3 0 0).

Fig. 7 displays the SEM micrographs of an uncovered substrate and of a monolayer coating that shows a smooth surface composed by hardly distinguishable particles. The EDS analysis confirms the presence of calcium and phosphorous throughout the film. The topography of the films has been determined by SFM and shows that the surface of the coatings is composed by aggregates between 1 and 2 μm of smaller crystals with valleys between them of around 250 nm. The roughness can be estimated at around 0.14 μm rms (root mean square).The thickness values range from around 1–4 μm for one (Fig. 8) and four (not shown) coatings layers, respectively. Consequently, it can be assumed that each deposition cycle yields about 1 μm of thickness.

The immersion in SBF shows the appearance of the first hints of bioactivity within 7 days of soaking although only after 15 days the substrate is completely covered. Fig. 7c shows the morphology of the apatite layer, composed by aggregates of needle-like crystallites, grown onto the chitosan apatite coating at two different magnifications. The EDS analysis confirms that the composition of the apatite layer grown onto the covered substrate resemble that of the underlying chitosan/apatite layer. In fact, due to the characteristics of this layer, it is very difficult to discern by XRD or FTIR the evidence of a newly formed apatite layer after the immersion in SBF.

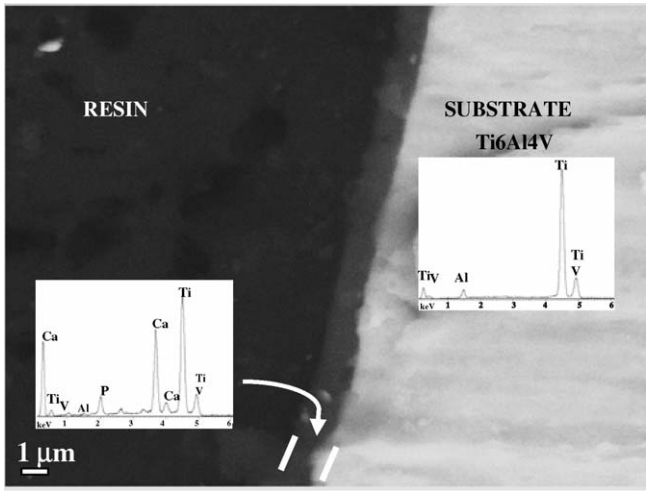

Fig. 8. SEM micrograph of one coating cross-section. EDS analysis of the layer and the substrate are included in the micrography.

The adhesion test shows values superior to 15 MPa, strength at which breakage occurs in the glue, in the interface glue/coating or between the substrate and the metallic holder; in no case fracture of the coating is observed. These minimum tensile strength adhesion values are comparable to those obtained for calcium phosphate coatings prepared by sol–gel technique,[57,58] electrodeposition,[59] plasma spray[60] or pulsed laser deposition.[34]

4. Conclusions

The following achievements can be remarked from the research described in this work:

- The synthetic route employed is simple, low cost and short time consuming.
- The precursors employed are costless and do not leave any harmful residues.
- The different procedure steps are carried out at room temperature.
- Powders with a wide chitosan/inorganic ratio can be easily prepared in large amounts.
- Adherent coatings are deposited onto Ti6Al4V substrates.

Considering all these reasons, this work opens many possibilities in the preparation of materials loaded with thermally instable substances such as antibiotics, growth factors, adhesion peptides and, even, cells. This fact could be of great interest in the case of layers, with the added value of ability to coat of coating intricate and thermally labile substrates.

Acknowledgements

Financial support of CICYT, Spain, through research project MAT2005-01486 is acknowledged. We also thank A. Rodriguez (Electron Microscopy Centre, Complutense University) and F. Conde (C.A.I. X-ray Diffraction Centre, Complutense University), for valuable technical and professional assistance. The substrate rods were kindly provided by Biomet Spain Orthopaedics.

References

1. Muzarelli, C. and Muzzarelli, R. A. A., Natural and artificial chitosan-inorganic composites. *J. Inorg. Biochem.*, 2002, **92**, 89–94.
2. Khor, E. and Lim, L. Y., Implantable applications of chitin and chitosan. *Biomaterials*, 2003, **24**, 2339–2349.
3. Suh, J. K. F. and Matthew, H. W. T., Application of chitosan-based polysaccharide biomaterials in cartilage tissue engineering: a review. *Biomaterials*, 2000, **21**, 2589–2598.
4. Synowiecki, J. and Al-Khateeb, N., Production, properties, and some new applications of chitin and its derivatives. *Crit. Rev. Food Sci. Nut.*, 2003, **43**, 145–171.
5. Dutta, P. K., Kumar, M. N. V. R. and Dutta, J., Chitin and chitosan for versatile applications. *J. Macromol. Sci. Pol. Rev.*, 2002, **C42**, 307–354.
6. Sinha, V. R., Sinha, A. K., Wadhawan, S., Kaushik, R., Kumira, R., Bansal, K. *et al.*, Chitosan microspheres as potential carrier for drugs. *Int. J. Pharm.*, 2004, **274**, 1–33.
7. Sashiwa, H. and Aiba, S.-I., Chemically modified chitin and chitosan as biomaterials. *Prog. Polym. Sci.*, 2004, **29**, 887–908.
8. Dodane, V. and Vilivalam, V. D., Pharmaceutical applications of increase in paracellular transport of macromolecular chitosan. *Pharm. Sci. Technol. Today*, 1998, **1**, 246–253.
9. Agnihotri, S. A., Mallikarjuna, N. N. and Aminabhavi, T. M., Recent advances on chitosan-based micro- and nanoparticles in drug delivery. *J. Control. Release*, 2004, **100**, 5–28.
10. Risbud, M., Endres, M., Ringe, J., Bhonde, R. and Sittinger, M., Biocompatible hydrogel supports the growth of respiratory epithelial cells: possibilities in tracheal tissue engineering. *J. Biomed. Mater. Res.*, 2001, **56**, 120–127.
11. Lahiji, A., Sohrabi, A., Hungerford, D. S. and Frondoza, C. G., Chitosan supports the expression of extracellular matrix proteins inhuman osteoblast and chondrocytes. *J. Biomed. Mater. Res.*, 2000, **51**, 586–595.
12. Yuan, Y., Zhang, P., Yang, Y., Wang, X. and Gu, X., The interaction of Schwann cells with chitosan membranes and fibers in vitro. *Biomaterials*, 2004, **25**, 4273–4278.
13. Yoshida, A., Miyazaki, T., Ishida, E. and Ashizuka, M., Preparation of bioactive chitosan-hydroxyapatite nanocomposites for bone repair through mechanochemical reaction. *Mater. Trans.*, 2004, **45**, 994–998.
14. Ito, M., Hidaka, Y., Nakajima, M., Yagasaki, H. and Kafrawy, A. H., Effect of hydroxyapatite content on a physical properties and connective tissue reactions to a chitosan-hydroxyapatite composite membrane. *J. Biomed. Mater. Res.*, 1999, **45**, 204–208.
15. Varma, H. K., Yokogawa, Y., Espinosa, F. F., Kawamoto, Y., Nishizawa, K., Nagata, F. *et al.*, Porous calcium phosphate coating over phosphorylated chitosan film by a biomimetic method. *Biomaterials*, 1999, **20**, 879–884.
16. Murugan, R. and Ramakrishna, S., Bioresorbable composite bone paste using polysaccharide based nano hydroxyapatite. *Biomaterials*, 2004, **25**, 3829–3835.
17. Xua, H. H. K. and Simon Jr., C. G., Fast setting calcium phosphate–chitosan scaffold: mechanical properties and biocompatibility. *Biomaterials*, 2005, **26**, 1337–1348.
18. Yokoyama, A., Yamamoto, S., Kawasaki, T., Kohgo, T. and Nakasu, M., Development of calcium phosphate cement using chitosan and citric acid for bone substitute materials. *Biomaterials*, 2002, **23**, 1091–1101.
19. Zhao, F., Yin, Y., Lu, W. W., Leong, J. C., Zhang, W., Zhang, J. *et al.*, Preparation and histological evaluation of biomimetic 3-D hydroxyapatite/chitosan gelatin network composite scaffolds. *Biomaterials*, 2002, **23**, 3227–3234.
20. Zhang, Y. and Zhang, M., Calcium/phosphate composite scaffolds for controlled in vitro antibiotic drug release. *J. Biomed. Mater. Res.*, 2002, **62**, 378–386.
21. Zhang, Y. and Zhang, M., Microstructural and mechanical characterization of chitosan scaffolds reinforced by calcium phosphates. *J. Non-Cryst. Solids*, 2001, **282**, 159–164.
22. Yin, Y., Ye, F., Cui, J., Zhang, F., Li, X. and Yao, K., Preparation and characterization of macroporous chitosan–gelatin/β-tricalcium phosphate composite scaffolds for bone tissue engineering. *J. Biomed. Mater. Res.*, 2003, **67A**, 844–855.
23. Sivakumar, M., Manjubala, I. and Panduranga Rao, K., Preparation, characterization and in-vitro release of gentamicin from coralline hydroxyapatite-chitosan composite microspheres. *Carbohydr. Polym.*, 2002, **49**, 281–288.
24. Sunny, M. C., Ramesh, P. and Varma, H. K., Microstructured microspheres of hydroxyapatite bioceramic. *J. Mater. Sci. Mater. Med.*, 2002, **13**, 623–632.
25. Paul, W. and Sharma, C. P., Development of porous spherical hydroxyapatite granules: application towards protein delivery. *J. Mater. Sci. Mater. Med.*, 1999, **10**, 383–388.
26. Yamaguchi, I., Tokuchi, K., Fukuzaki, H., Koyama, Y., Takakuda, K., Monma, H. *et al.*, Preparation and microstructure analysis of chitosan/hydroxyapatite nanocomposites. *J. Biomed. Mater. Res.*, 2001, **55**, 20–27.
27. Yokogawa, Y., Nishizawa, K., Nagata, F. and Kameyama, T., Bioactive properties of chitin/chitosan–calcium phosphate composite materials. *J. Sol-Gel Sci. Technol.*, 2001, **21**, 105–113.
28. Tachaboonyakiat, W., Serizawa, T. and Akashi, M., Hydroxyapatite formation on/in biodegradable chitosan hydrogels by an alternate soaking process. *Polym. J.*, 2001, **33**, 177–181.
29. Tachaboonyakiat, W., Serizawa, T. and Akashi, M., Inorganic–organic polymer hybrid scaffold for tissue engineering—II: partial enzymatic degrada-

tion of hydroxyapatite–chitosan hybrid. *J. Biomater. Sci. Polym. Edn.*, 2002, **13**, 1021–1032.
30. Hu, Q., Li, B., Wang, M. and Shen, J., Preparation and characterization of biodegradable chitosan/hydroxyapatite nanocomposite rods via in situ hybridization: a potential material as internal fixation of bone fracture. *Biomaterials*, 2004, **25**, 779–785.
31. Weng, W., Han, G., Du, P. and Shen, G., The effect of citric acid on sol–gel preparation of apatite films. *Mater. Chem. Phys.*, 2002, **77**, 578–582.
32. Sun, L., Berndt, C. C., Gross, K. A. and Kucuk, A., Material fundamentals and clinical performance of plasma-sprayed hydroxyapatite coatings: a review. *J. Biomed. Mater. Res.*, 2001, **58**, 570–592.
33. Yang, Y., Kim, K.-H. and Ong, J. L., A review on calcium phosphate coatings produced using a sputtering process—an alternative to plasma spraying. *Biomaterials*, 2005, **26**, 327–337.
34. García-Sanz, F. J., Mayor, M. B., Arias, J. L., Pou, J., León, B. and Pérez-Amor, M., Hydroxyapatite coatings: a comparative study between plasma-spray and pulsed laser deposition techniques. *J. Mater. Sci. Mater. Med.*, 1997, **8**, 861–865.
35. Lewis, G., Hydroxyapatite-coated bioalloy surfaces: current status and future challenges. *Bio-Med. Mater. Eng.*, 2000, **10**, 157–188.
36. Daculsi, G., Laboux, O. and LeGeros, R. Z., Outcome and perspectives in bioactive coatings: what's new, what's coming. *ITBM-RBM*, 2002, **23**, 317–325.
37. Yan, W.-Q., Nakamura, T., Kawanabe, K., Nishigochi, S., Oka, M. and Kokubo, T., Apatite layer-coated titanium for use as bone bonding implants. *Biomaterials*, 1997, **18**, 1185–1190.
38. Mao, C., Li, H., Cui, F., Ma, C. and Feng, Q., Oriented growth of phosphates on polycrystalline titanium in a process mimicking biomineralization. *J. Cryst. Growth*, 1999, **206**, 308–321.
39. Li, P., Biomimetic nanoapatite coating capable of promoting bone ingrowth. *J. Biomed. Mater. Res.*, 2003, **66A**, 79–85.
40. Li, F., Feng, Q. L., Cui, F. Z., Li, H. D. and Schubert, H., A simple biomimetic method for calcium phosphate coating. *Surf. Coat. Technol.*, 2002, **154**, 88–93.
41. Wang, J., Nayrolle, P., Stigter, M. and de Groot, K., Biomimetic and electrolytic calcium phosphate coatings on titanium alloy: physicochemical characteristics and cell attachment. *Biomaterials*, 2004, **25**, 583–592.
42. Kim, H.-M., Kim, Y., Park, S.-J., Rey, C., Lee, H. M., Glimcher, M. J. *et al.*, Thin film of low crystalline calcium phosphate apatite formed at low temperature. *Biomaterials*, 2000, **21**, 1129–1134.
43. Kumar, M., Dasarathy, H. and Riley, C., Electrodeposition of brushite coatings and their transformation in aqueous solutions. *J. Biomed. Mater. Res.*, 1999, **45**, 302–310.
44. Han, Y., Fu, T., Lu, J. and Xu, K., Characterization and stability of hydroxyapatite coatings prepared by an electrodeposition and alkaline-treatment process. *J. Biomed. Mater. Res.*, 2001, **54**, 96–101.
45. Redepenning, J., Venkataraman, G., Chen, J. and Stafford, N., Electrochemical preparation of chitosan/hydroxyapatite composite coatings on titanium substrates. *J. Biomed. Mater. Res.*, 2003, **66A**, 411–416.
46. Stigter, M., Bezemer, J., de groot, K. and Layrolle, P., Incorporation of different antibiotics into carbonated hydroxyapatie coatings on titanium implants, release and antobiotic efficacy. *J. Control. Release*, 2004, **99**, 127–137.
47. Stigter, M., de Groot, K. and Layrolle, P., Incorporation of tobramycin into biomimetic hydroxyapatite coating on titanium. *Biomaterials*, 2002, **23**, 4143–4153.
48. Radin, S., Campbell, J. T., Ducheyne, P. and Cuckler, J. M., Calcium phosphate ceramic coatings as carriers of vancomycin. *Biomaterials*, 1997, **18**, 777–782.
49. Campbell, A. A., Song, L., Li, X. S., Nelson, B. J., Bottoni, C., Brooks, D. E. *et al.*, Development, characterization, and anti-microbial efficacy of hydroxiapatite–chlorhexidine coatings produced by surface-induced mineralization. *J. Biomed. Mater. Res. (Appl. Biomater.)*, 2000, **53**, 400–407.
50. Kokubo, T., Kushitani, H., Ohtsuki, C., Sakka, S. and Yamamuro, T., Solutions able to reproduce in vivo surface-structure changes in bioactive glass-ceramic A-W. *J. Biomed. Mater. Res.*, 1990, **24**, 721–734.
51. American Society for Testing Materials, *Specifications for calcium phosphate coating for implantable materials Section 13*. Medical devices. Easton MD: 2001 Annual book of ASTM standard.
52. Van de Velde, K. and Kiekens, P., Structure analysis and degree of substitution of chitin, chitosan and dibutyrylchitin by FT-IR spectroscopy and solid state ^{13}C NMR. *Carbohydr. Polym.*, 2004, **58**, 409–416.
53. Fowler, B. O., Infrared studies of apatites, vibrational assigments for calcium, strontium and barium hydroxyapatites utilizing isotopic substitution. *Inorg. Chem.*, 1974, **13**, 194–207.
54. Rey, C., Collins, B., Goehl, T., Dickson, R. and Glimcher, M. J., The carbonate enviroment in bone mineral: a resolution-enhanced fourier transform infrared spectroscopy study. *Calcif. Tissue Int.*, 1989, **45**, 157–164.
55. Yamaguchi, I., Iizuka, S., Osaka, A. and Monma, H., Tanaka The effect of citric acid on chitosan/hydroxyapatite composites. *J. Colloids Surf. A*, 2003, **214**, 111–118.
56. Van der Houwen, J. A. M., Cressey, G., Cressey, B. A. and Valsami-Jones, E., The effect of organic ligands on the crystallinity of calcium phosphate. *J. Cryst. Growth*, 2003, **249**, 572–583.
57. Weng, W. and Baptista, J. L., Preparation and characterization of hydroxyapatite coatings on Ti6Al4V alloy by sol–gel method. *J. Am. Ceram. Soc.*, 1999, **82**, 27–32.
58. Liu, D.-M., Yang, Q. and Troczynski, T., Sol–gel hydroxyapatite coatings on stainless steel substrates. *Biomaterials*, 2002, **23**, 691–698.
59. Lin, S., LeGeros, R. Z. and LeGeros, J. P., Adherent octacalciumphosphate coating on titanium alloy using modulated electrochemical deposition method. *J. Biomed. Mater. Res.*, 2003, **66A**, 819–828.
60. Gu, Y. W., Khor, K. A. and Cheang, P., In vitro studies of plasma-sprayed hydroxyapatite/Ti-6Al-4V composite coatings in simulated body fluid (SBF). *Biomaterials*, 2003, **24**, 1603–1611.